Modeling Monovalent Selective Electrodialysis for Selective Nutrient Recovery from Spanish Groundwater

Vinn Nguyen

Lienhard Research Group

Summer 2024

1. Introduction

In regions with heavy agriculture, water quality and scarcity are increasingly critical issues that arise due to overexploitation of natural resources. The Campo de Cartagena basin in southeastern Spain is a prominent example, where extensive agricultural activities have led to overuse and pollution of groundwater [1, 2, 3, 4, 5]. The water present in the Campo de Cartagena basin contains high levels of monovalent ions detrimental to crop growth (Na^+ and Cl^-), making it unsuitable for direct irrigation use. However, this water is also rich in divalent ions that serve as crop nutrients (Mg^{2+}, Ca^{2+}, and SO_4^{2-}).

Monovalent selective electrodialysis (MSED) has emerged as a promising method for the selective removal of ions that are detrimental to crops (e.g., Na^+ and Cl^-) while retaining essential nutrients (e.g., Mg_2^+, Ca_2^+, and SO_4^{2-}) in the water. Unlike traditional reverse osmosis (RO), which indiscriminately removes both beneficial and harmful ions, MSED offers a more tailored approach to water treatment that aligns with the specific needs of agricultural irrigation [6]. MSED is a specialized water treatment derivative of electrodialysis that uses an electric field to separate monovalent ions from multivalent ions through ion-exchange membranes that are specialized for selectivity. These membranes allow monovalent ions to pass more easily due to their smaller size and lower charge density, while rejecting multivalent ions, which have larger hydration shells and stronger interactions with the membrane [7].

My research focused on modifying and including additional functionality to an existing semi-empirical multi-ion MSED transport model. The main objective was to adapt the model for a new application: treating brackish groundwater to produce an irrigation product, rather than its original use for lithium extraction. This involved making necessary modifications to the model, incorporating new experimental data, and generating visual representations of the trends observed for analysis.

2. Methods

2.1 Relevant Equations

The transport number is used to assess the proportion of utilization of current by individual ions within the MSED system. It is defined with the following equation:

$$T_j^{cp} = \frac{\Delta w_j F}{i \Delta t N_{cp}} \quad (1)$$

Where$j$ is the ion, Δw_j is the change in the weight of ion j after time Δt, F is faraday's constant, N_{cp} is the number of cell pairs.

The normalized transport number is used to assess the proportion of utilization of current by individual ions within the MSED system, relative to its initial concentration. It is defined with the following equation:

$$T_i^{norm} = \frac{T_i}{C_i(0)} \quad (2)$$

where i is the relevant ion, T_i is the transport number, $C_i(0)$ is the initial concentration and $T_i^{norm}$is the normalized transport number.

The ion-ion selectivity factor quantifies the membrane's ability to differentiate between two different ions. It is defined with the following equation:

$$SF_{ij} = \frac{T_i}{C_i(0)} / \frac{T_j}{C_j(0)} \quad (3)$$

where i is the ion with higher permeability, j is the ion with lower permeability, and SF_{ij} is the selectivity factor that quantifies the separation. $C_i(0)$ and $C_j(0)$ are the initial

concentrations of ions i and j, respectively. T_i and T_j are transport numbers.

The effective selectivity factor measures a membrane's overall ability to differentiate between groups of ions. It is defined with the following equation:

$$SF = \frac{\Sigma T_m}{\Sigma C_m(0)} \Big/ \frac{\Sigma T_d}{\Sigma C_d(0)} \quad (4)$$

where m are monovalent ions, d are divalent ions, and SF is the selectivity factor that quantifies the separation. $\Sigma C_m(0)$ and $\Sigma C_d(0)$ are the sum of initial concentrations of monovalent and divalent ions, respectively. ΣT_m and ΣT_d are the sum of transport numbers.

Power consumption quantifies the rate at which electrical energy is being used to drive a process. It is defined with the following equation:

$$P(t) = I \bullet V(t) \quad (5)$$

Where $P(t)$ is power, I is current, and $V(t)$ is voltage.

2.2 Code Overview

The ion transport model in the present study simulates the dynamic behavior of ions and water molecules in a monovalent selective electrodialysis (MSED) stack. To run the model successfully it is essential to configure and initialize it with a range of critical parameters and constants which are defined by the user. Key parameters such as operational conditions (pressure and temperature), initial flow rate, stack dimensions, initial solution properties (salinity and molality), and pertinent constants (Faraday's constant, Boltzmann constant, etc.) are defined. Following this, the selectivity parameters of the ions, including permeabilities, valances, and molecular weight are specified. The system is then configured with specific MSED operation parameters, such as the number of cell pairs, driving forces, and integrator details.

After the relevant constants are initialized, experimental data, including normalized ion concentrations (in the dilute stream) versus time, initial ion concentrations, electrical current, and voltages versus time, are read. The code only utilizes concentration data until the time point where Cl^- and Na^+ fall below their respective toxicity limits. Then a matrix is initialized to store calculated flux values of ions over time, computed by iterating through the time steps of the experimental data and calculating the difference in ion concentrations between the initial and subsequent time steps. The mean ion flux is then computed, providing a baseline for subsequent optimization steps.

The next major step in the code involves optimizing the transport numbers[1]. An initial guess for the transport numbers is provided, and the code defines an objective function that compares the experimentally determined mean ion flux with the modeled flux. After the objective function is minimized, these transport numbers are calculated (equation 1) and stored for a given set of operating conditions. They are also normalized with respect to the initial ion concentrations, and the normalized values are saved (see equation 2 above). Following the optimization, the code calculates selectivity factors for the system, specifically focusing on the selectivity between monovalent and divalent ions as well as with specific ion pairs (see equations 3 & 4 above).

The code then simulates the transient behavior of ion concentrations over time using the optimized transport numbers. It initializes a time vector and an array to store the transient concentrations, iteratively updating these concentrations based on the calculated fluxes. If any ion concentration drops to zero, the code adjusts the transport numbers to maintain physical accuracy, ensuring that concentrations remain non-negative. The normalized transient concentrations are then visualized, showing how each ion's concentration changes over time. Alongside the ion transport simulation, the code also performs energy calculations, utilizing experimental voltage data and calculating the cumulative and mean power consumption (see equation 5 above).

2.3 Contributions

[1] The transport number is a fraction of the total electric current carried by an ion.

In my work, I adapted the existing MSED transport model to accommodate for the seven target ions: Na^+, K^+, Mg^{2+}, Ca^{2+}, Cl^-, NO_3^-, SO_4^{2-}. This required updating and implementing key initialization constants and ion-specific properties, including molecular weight vectors and ionic valencies. I also modified the optimization parameters, fine-tuning the search space and initial guesses. Additionally, I adjusted the data file directory to ensure proper reading and incorporation of the experimental data.

Once the model was correctly configured for the seven ions, I implemented CSV truncation to pre-process the data and identify experiments that produced viable irrigation products. For a set of 6 experiments, I completed the following steps. First, I calculated transport numbers and then divided it by its initial concentration to get normalized transport numbers using equation 1 & 2, allowing for a less biased comparison between different ions than using the transport numbers. I then calculated the ion-ion selectivity factor for the following ion pairs: Na^+/Ca^{2+}, Na^+/Mg^{2+}, Na^+/K^+, Cl^-/SO_4^{2-}, and NO_3^-/Cl^- using equation 3. Furthermore, I determined the effective selectivity factors for monovalent/divalent separation, monovalent/divalent anion separation, and monovalent/divalent cation separation using equation 4. Finally, I calculated the power consumption for each experiment using equation 5. I saved all the calculations in csv files and developed a graphing script to plot them.

3. Results and Discussion

3.1 Normalized Concentration

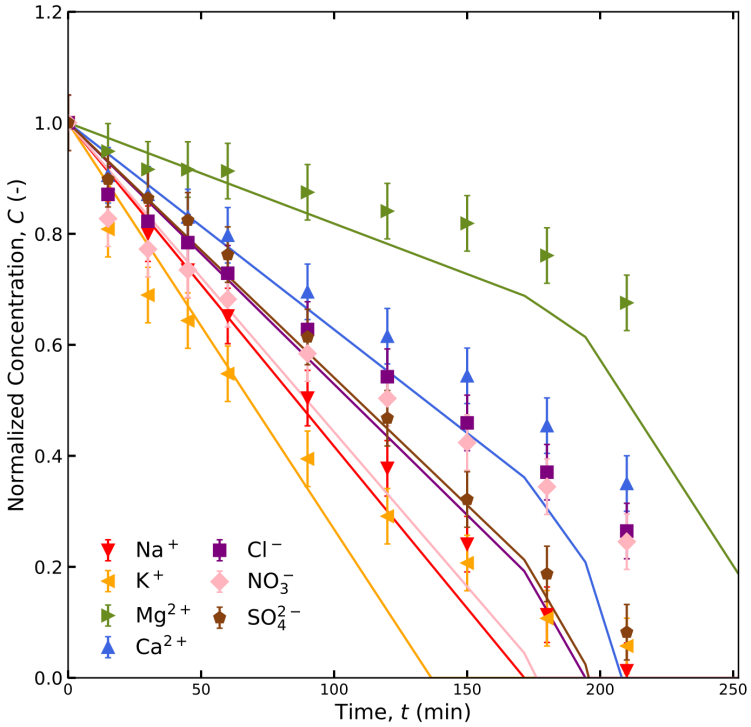

Figure 1: Normalized concentrations as a function of time at 0.1 Ampere (applied current density) for studied ions in the artificial brackish groundwater

Figures 1 through 6 show the normalized ion concentrations in the diluate stream versus time for six different experiments, each with a different applied current[2]. The monovalent ions (Na^+, K^+, Cl^-, and NO_3^-) show a more rapid decline in normalized concentration compared to divalent ions. Among these, K^+ exhibits the steepest decline, indicating the fastest normalized rate of transport. In contrast, the divalent ions (Mg^{2+}, Ca^{2+}, and SO_4^{2-}) show a noticeably slower reduction in concentration over time. This slower decrease aligns with the generally lower mobility of divalent ions, which is likely due to their higher charge and stronger interaction (both attraction and repulsion) with the membrane. Mg^{2+} and Ca^{2+} exhibit similar trends, but Mg^{2+} consistently shows a

[2] Figures 2 through 6 can be found in Appendix A.

slightly lower slope. The difference in removal rate between monovalent and divalent ions gets increasingly pronounced as the current increases noted by Figure 6 (see Appendix A).

Another notable trend is the generally faster removal of cations compared to anions. Specifically, for monovalent ions, the normalized concentrations of Cl^- and NO_3^- decrease at a slower rate than those of Na^+ and K^+ across all experiments. However, within the divalent ions, SO_4^{2-} is removed more rapidly than both Mg^{2+} and Ca^{2+}, highlighting a unique behavior. Additionally, as current increases, all normalized concentrations for every ion rapidly decline at a faster rate.

3.2 Transport Numbers

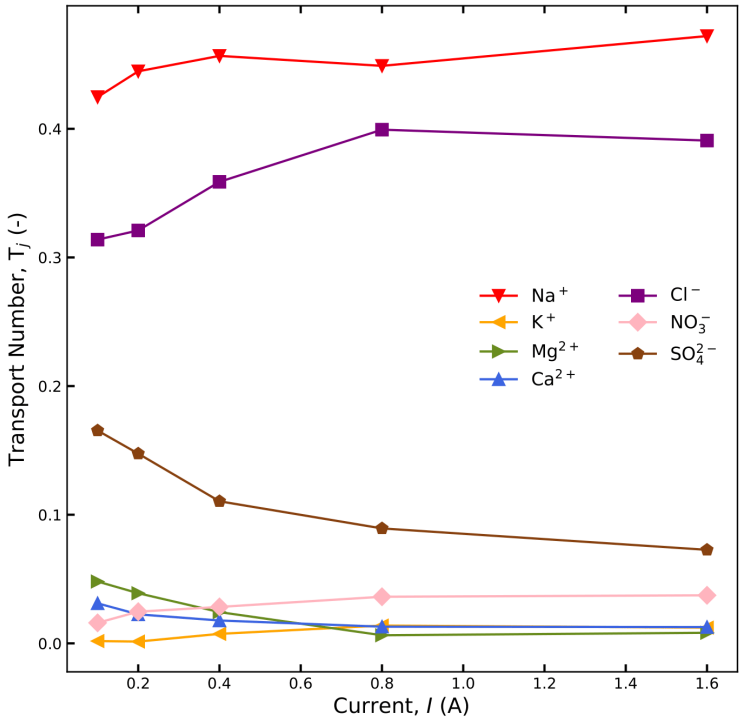

Figure 7: Transport numbers as a function of current for studied ions in the artificial brackish groundwater

Figure 7 shows transport numbers for each ion with increasing applied

experimental current. Across all experiments, Na^+ has the largest transport number followed by Cl^- and SO_4^{2-}. A possible reason for this trend is because Cl^-, SO_4^{2-}, and Na^+ (ordered in increasing concentration) make up 88% of the initial mass concentrations of ions resulting in these ions contributing the largest fraction of the total electric current. Despite Cl^- and SO_4^{2-} individually having higher initial mass concentrations, both exhibit lower individual transport numbers than Na^+. Additionally, as the current increases, the transport numbers of monovalent ions rise, while those of divalent ions decline.

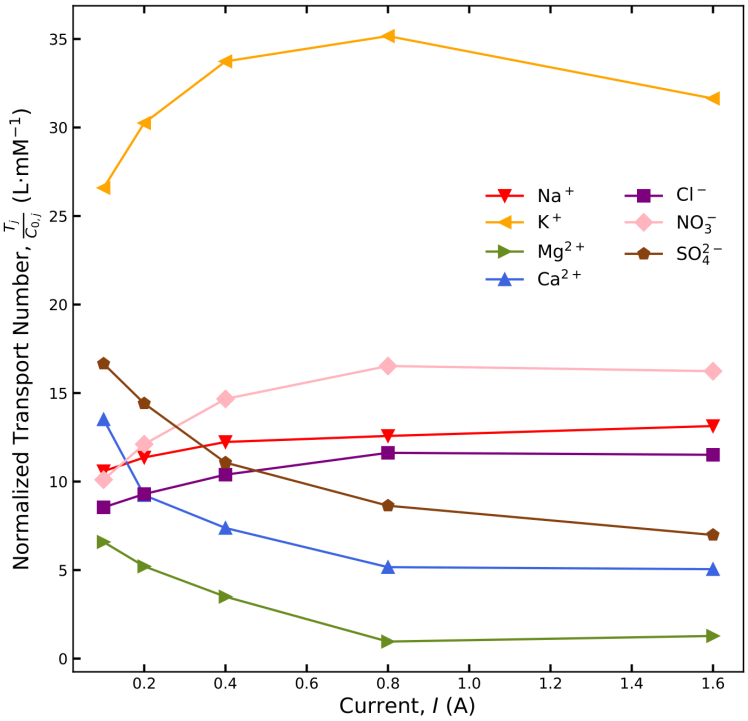

Figure 8: Plot of normalized transport number with respect to initial concentration for all studied ions as a function of current

Figure 8 reveals that K^+ has the highest normalized transport number, indicating that, relative to its initial concentration, K^+ contributes the largest fraction of the total electric current among the seven ions. This suggests that K^+ is transported more efficiently through the membrane compared to other ions. At lower currents, monovalent and divalent ions have similar transport numbers. However, as the current increases,

monovalent transport numbers rise, while those of divalent ions decrease, resulting in all three divalent ions having the lowest transport numbers.

3.3 Selectivity

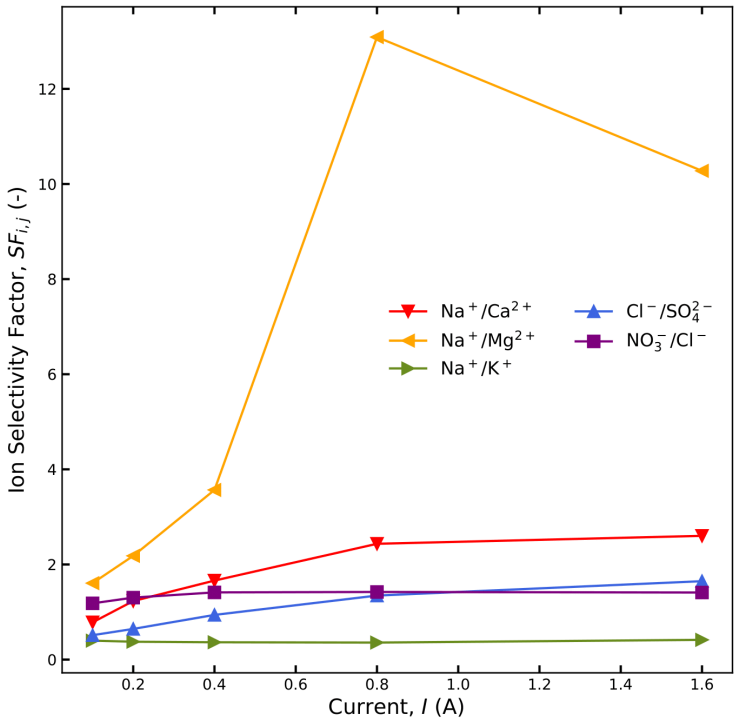

Figure 9: Plot of Ion-Ion selectivity factors for five ion pairs (Na^+/Ca^{2+}, Na^+/Mg^{2+}, Na^+/K^+, Cl^-/SO_4^{2-}, and NO_3^-/Cl^-) as a function of current

Ion-Ion selectivity factor was calculated for five ions pairs as shown in Figure 9. The highest selectivity factor was Na^+/Mg^{2+} indicating that the CEMs strongly preferred the passage of Na^+ relative to Mg^{2+}. This corroborates with the trends found in normalized concentrations versus time (Figs. 1-6) as Mg^{2+} was always the slowest decreasing ion. Additionally, Na^+ seemed to be slightly preferred over Ca^{2+} while being equally preferred with K^+. As for the other pairs, both Cl^- and NO_3^- were slightly preferred over their respective pairs of SO_4^{2-} and Cl^-.

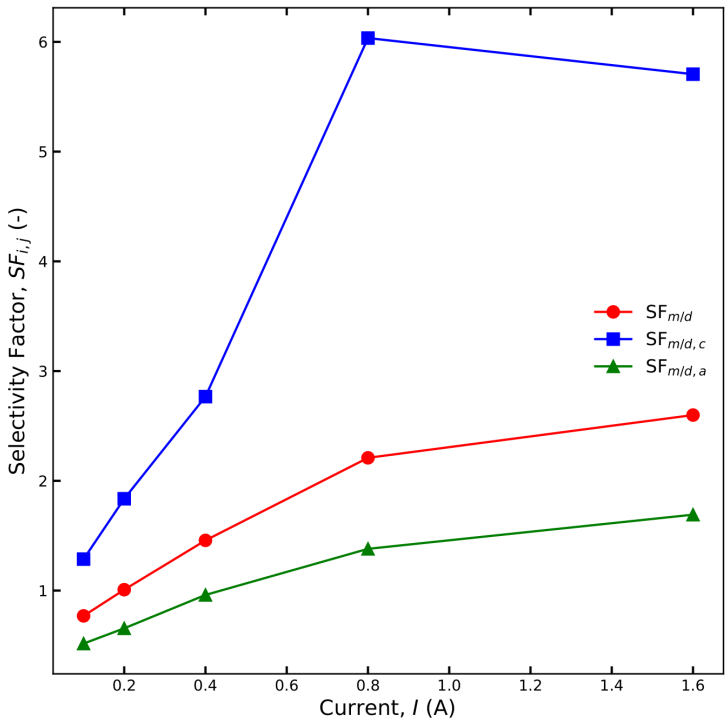

Figure 10: Plot of effective selectivity factors for monovalent and divalent ions as a function of current

Figure 10 illustrates the effective selectivity factor for three groups: all monovalent and divalent ions, monovalent and divalent cations, and monovalent and divalent anions. It highlights the Ion exchange membrane's (IEM) preference of monovalent ions to divalent ions. It is apparent that the effective selectivity factor for monovalent and divalent cations is comparatively very large relative to that of the anions, illuminating the cation exchange membrane's (CEM) particular effectiveness at differentiating between monovalent and divalent ions, which is valuable for targeted ion removal. On the other hand the anion exchange membrane (AEM) is not as effective in separating monovalent and divalent anions. As current increases, so does the selectivity factor indicating that separation is more effective at higher currents. However it is noted that at the 0.1 - 0.2 current range, the effective separation factor for monovalent and divalent ions are generally less than one (especially for anions)

indicating that at lower currents, the membranes prefer the passage of divalents.

3.4 Power Consumption

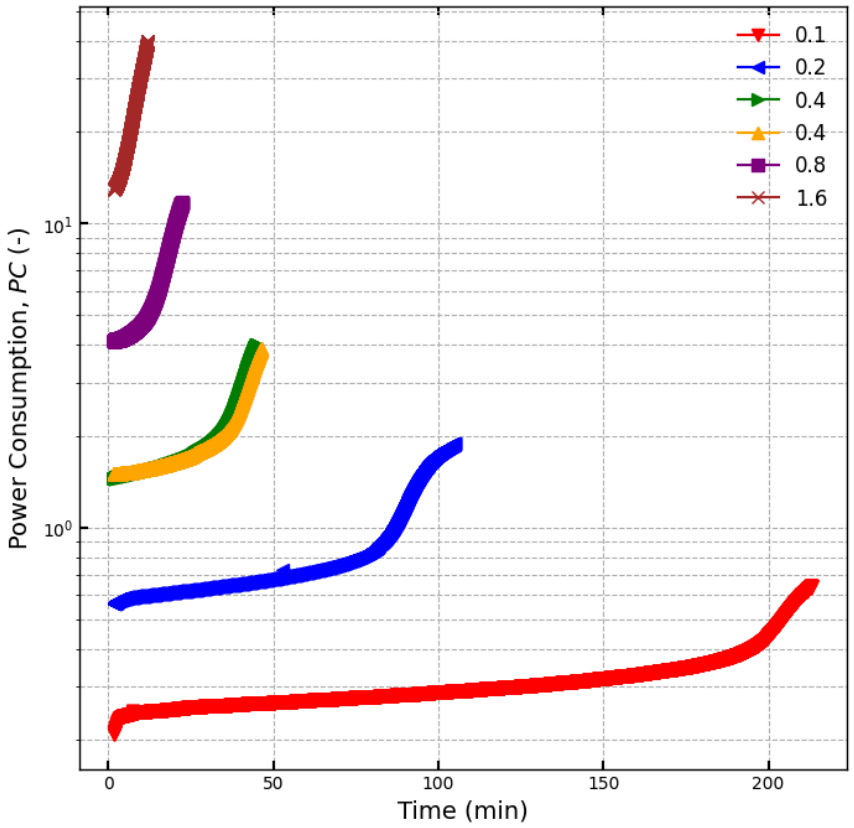

Figure 11: Plot of power consumption as a function of time for all experiments with a logarithmic y axis

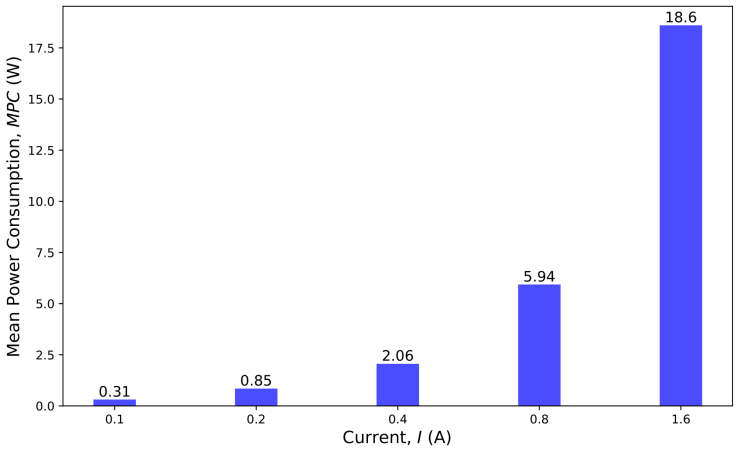

Figure 12: Plot of mean power consumption as a function of current for all experiments

Figure 11 illustrates the distinct temporal power consumption for each experiment. At 0.1 amps, power consumption shows a slow, gradually increasing exponential trend over 220 minutes. In contrast, at 1.6 amps, the power consumption experiences a rapid and sharp exponential rise within just 20 minutes. Figure 12 corroborates this trend by illustrating significant order-of-magnitude differences in mean power consumption.

4. Conclusion

In summary, I adapted the semi-empirical multi-ion MSED transport model to simulate the behavior of brackish groundwater treated for irrigation, allowing for a detailed analysis of trends observed in the experimental data. To do this I added functionality to the model to calculate, analyze, and plot transport numbers, selectivity factors, and power consumption.

The results of the simulations and analyses revealed the CEM more effectively separates monovalent and divalent cations relative to the AEM separation of anions. This preference was consistent across all current levels experimentally tested, suggesting that the MSED system is particularly effective at differentiating between monovalent and divalent ions, which is vital for optimizing the irrigation quality of treated water. Furthermore, calculated selectivity factors provide further insight into IEMs' ion differentiation capabilities, particularly their strong preference for Na^+ over divalent cations like Mg^{2+} and Ca^{2+}. Overall, this work advances our understanding of MSED technology's potential for treating brackish groundwater by illustrating and quantifying the CEM’s effectiveness and AEM’s usefulness at separating monovalent and divalent cations which is a useful insight in producing a nutrient-rich irrigation product.

5. Acknowledgements

I would like to sincerely thank PhD candidate Samuel Marcus Heath for being the world's greatest mentor.

Appendix A

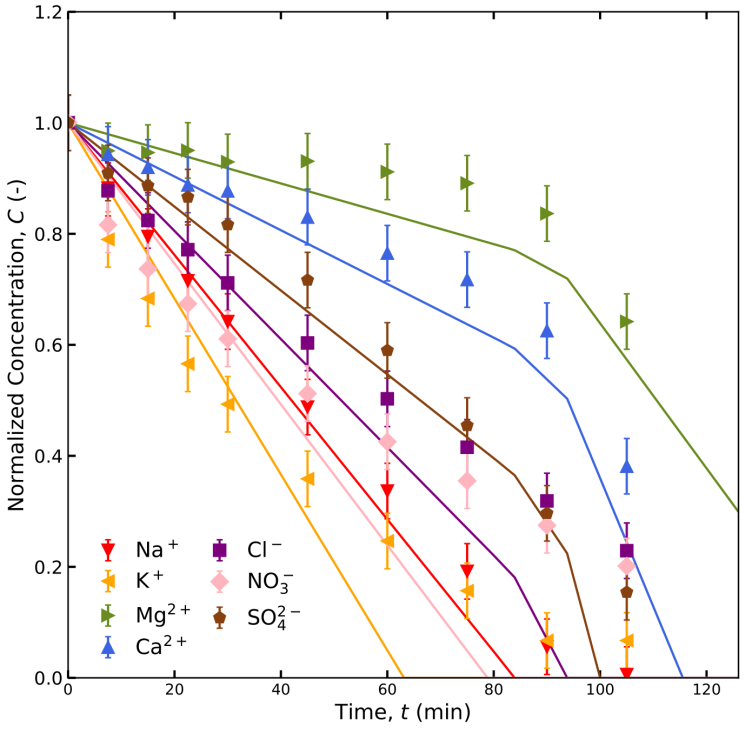

Figure 2: Plot of normalized concentrations for studied ions in the artificial brackish groundwater as a function of time at 0.2 Ampere

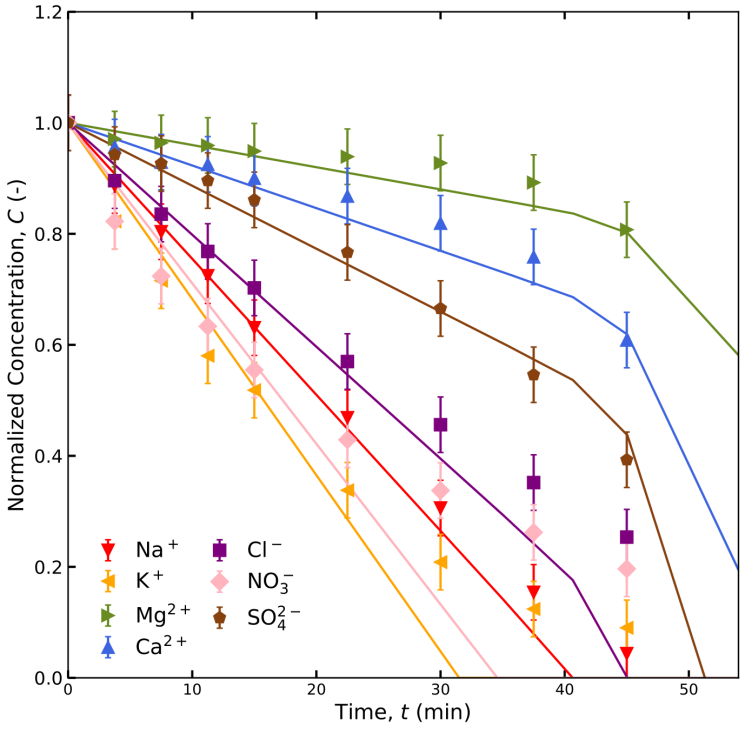

Figure 3: Plot of normalized concentrations for studied ions in the artificial brackish groundwater as a function of time at 0.4 Ampere

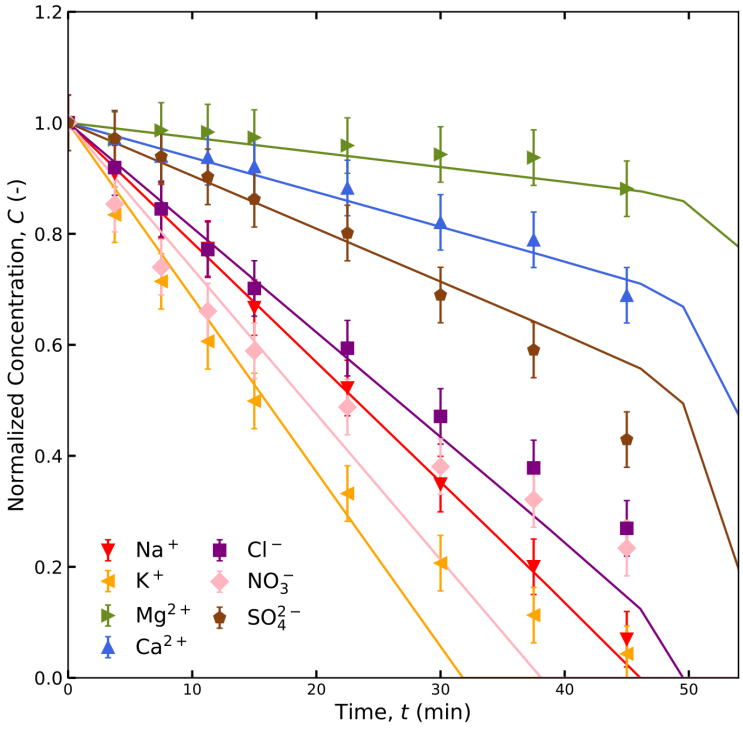

Figure 4: Plot of normalized concentrations for studied ions in the artificial brackish groundwater as a function of time at 0.4 Ampere - two experiments were run at 0.4 ampere

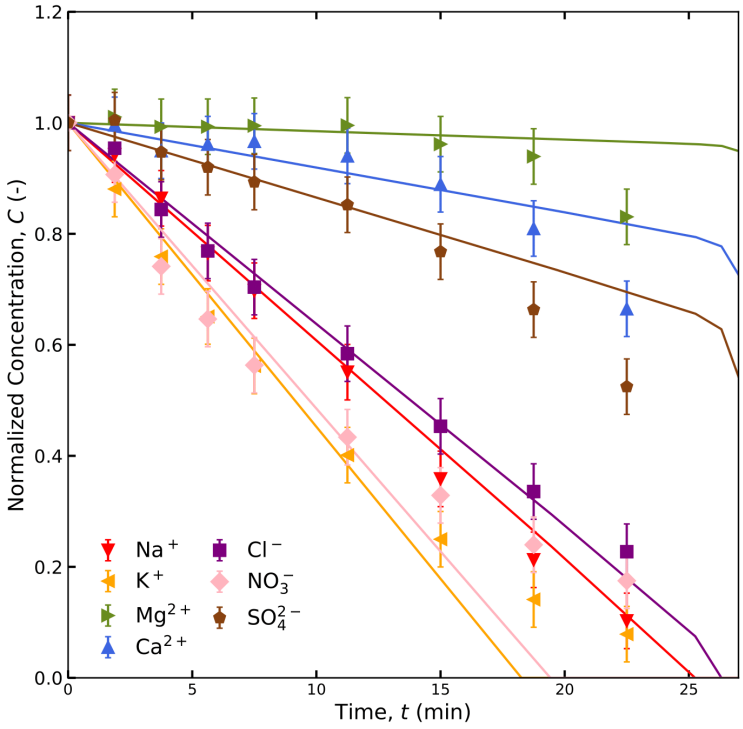

Figure 5: Plot of normalized concentrations for studied ions in the artificial brackish groundwater as a function of time at 0.8 Ampere

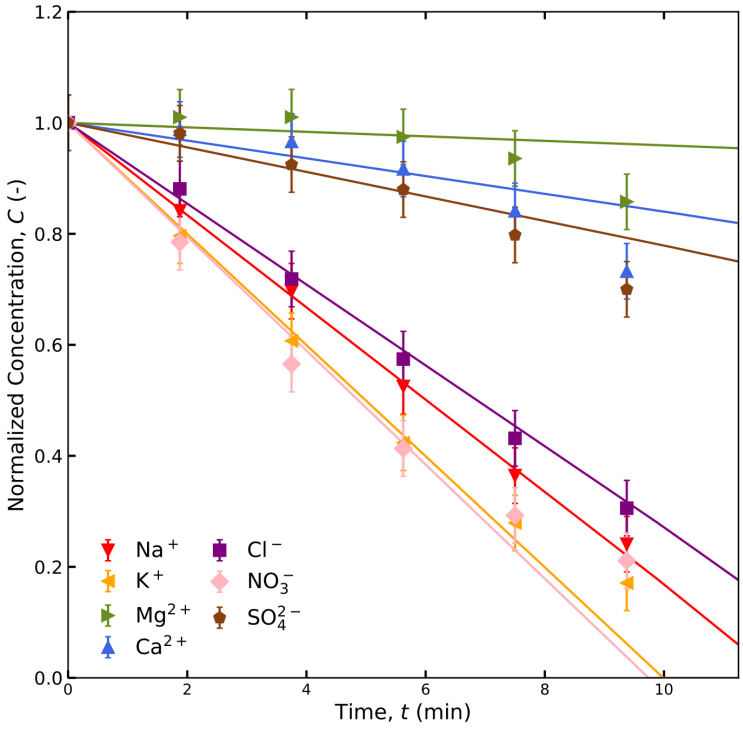

Figure 6: Plot of normalized concentrations for studied ions in the artificial brackish groundwater as a function of time at 1.6 Ampere

References

1. Baudron, P (2013). Anthropization of a semiarid Mediterranean multi-layer aquifer system (Campo de Cartagena, Se Spain). Hydrodynamic, geochemical and isotopic approaches. *PhD Thesis*, *1*, 1-226.

2. Conesa, H. M., & Jiménez-Cárceles, F. J. (2007). The Mar Menor lagoon (Se Spain): A singular natural ecosystem threatened by human activities. *Marine Pollution Bulletin*, *54*(7), 839–849.

3. Jiménez-Martínez, J., García-Aróstegui, J. L., Hunink, J. E., Contreras, S., Baudron, P., & Candela, L. (2016) The role of groundwater in highly human-modified hydrosystems: a review of impacts and mitigation options in the Campo de Cartagena-Mar Menor coastal plain (SE Spain). *Environmental Reviews*, *24*(4), 377–392.

4. Lloret, J., Marin, A., Marin-Guirao, L., & Velasco, J. (2005). Changes in macrophytes distribution in a hypersaline coastal lagoon associated with the development of intensively irrigated agriculture. *Ocean & Coastal Management*, *48*(9-10), 828–842.

5. Perez-Ruzafa, A., Marcos-Diego, C., & Ros, J. D. (1991). Environmental and biological changes related to recent human activities in the Mar Menor (SE of Spain). *Marine Pollution Bulletin*, *23*, 747–751.

6. Rehman, D., Ahdab, Y. D., & Lienhard, J. H. (2021). Monovalent selective electrodialysis: Modeling multi-ionic transport across selective membranes. Water Research, 199, 117171–117171. https://doi.org/10.1016/j.watres.2021.117171

7. Heath, S (2023). Treating Brackish Groundwater for Irrigation with Selective Electrodialysis and Nanofiltration. *Massachusetts Institute of Technology (MIT) Master's Thesis*